PRC2-mediated repression of SMARCA2 predicts EZH2 inhibitor activity in SWI/SNF mutant tumors

Thomas Januario[a,1], Xiaofen Ye[a,1], Russell Bainer[b], Bruno Alicke[c], Tunde Smith[a], Benjamin Haley[d], Zora Modrusan[d], Stephen Gould[c], and Robert L. Yauch[a,2]

[a]Department of Discovery Oncology, Genentech, Inc., South San Francisco, CA 94080; [b]Department of Bioinformatics, Genentech, Inc., South San Francisco, CA 94080; [c]Department of Translational Oncology, Genentech, Inc., South San Francisco, CA 94080; and [d]Department of Molecular Biology, Genentech, Inc., South San Francisco, CA 94080

Edited by Joan S. Brugge, Harvard Medical School, Boston, MA, and approved October 3, 2017 (received for review March 8, 2017)

Subunits of the SWI/SNF chromatin remodeling complex are frequently mutated in human cancers leading to epigenetic dependencies that are therapeutically targetable. The dependency on the polycomb repressive complex (PRC2) and EZH2 represents one such vulnerability in tumors with mutations in the SWI/SNF complex subunit, SNF5; however, whether this vulnerability extends to other SWI/SNF subunit mutations is not well understood. Here we show that a subset of cancers harboring mutations in the SWI/SNF ATPase, SMARCA4, is sensitive to EZH2 inhibition. EZH2 inhibition results in a heterogenous phenotypic response characterized by senescence and/or apoptosis in different models, and also leads to tumor growth inhibition in vivo. Lower expression of the SMARCA2 paralog was associated with cellular sensitivity to EZH2 inhibition in SMARCA4 mutant cancer models, independent of tissue derivation. SMARCA2 is suppressed by PRC2 in sensitive models, and induced SMARCA2 expression can compensate for SMARCA4 and antagonize PRC2 targets. The induction of SMARCA2 in response to EZH2 inhibition is required for apoptosis, but not for growth arrest, through a mechanism involving the derepression of the lysomal protease cathepsin B. Expression of SMARCA2 also delineates EZH2 inhibitor sensitivity for other SWI/SNF complex subunit mutant tumors, including SNF5 and ARID1A mutant cancers. Our data support monitoring SMARCA2 expression as a predictive biomarker for EZH2-targeted therapies in the context of SWI/SNF mutant cancers.

EZH2 | SMARCA4 | SMARCA2 | PRC2 | ARID1A

SWI/SNF, or BAF (Brg/Brahma-associated factors), complexes compose a family of ATP-dependent chromatin remodeling complexes that play critical roles in controlling gene transcription and DNA repair through their ability to regulate the accessibility of DNA in the nucleus (1, 2). In mammals, these complexes are composed of approximately 15 subunits, including either the SMARCA4 or SMARCA2 ATPase and additional core and accessory subunits whose specialized protein domains enable interactions with chromatin and/or DNA substrates. SWI/SNF complexes notably control lineage specification and differentiation programs in tissues, and these highly specific functions can be achieved through combinatorial subunit assembly, as well as tissue/lineage-specific expression of some subunits.

Large-scale cancer genome sequencing efforts have revealed that multiple SWI/SNF complex proteins are recurrently mutated in ~20% of human cancers (3). Mutations often render the encoded protein nonfunctional and associate with unique tumor spectra, suggesting distinct tumor-suppressor functions across these cancers. For example, the SWI/SNF complex subunit SNF5 is subject to biallelic mutational inactivation in nearly all malignant rhabdoid tumors (MRTs), and studies in genetically engineered mouse models of SNF5 inactivation have supported its role as a bona fide tumor suppressor (3–6). Similarly, recurrent inactivating mutations in additional BAF subunits have been identified in other indications, including *ARID1A* mutations in ovarian clear-cell and endometroid cancers, as well as hepatocellular and gastric cancers. *SMARCA4* mutations likewise are observed across a spectrum of cancers of the lung and bladder, and nearly all small cell carcinomas of the ovary, hypercalcemic-type (SCCOHT) (3, 7–9). Although the mechanisms underlying tumorigenesis in these specific contexts have yet to be fully elucidated, data are further supportive of a tumor-suppressive function (10, 11).

Efforts to therapeutically target SWI/SNF-defective cancers have focused on identifying novel vulnerabilities that may be a consequence of the altered chromatin state caused by mutations in BAF complex subunits. One such described vulnerability was based on the initial discovery in *Drosophila* of an opposing and antagonistic role of BAF and polycomb complexes in regulating gene expression (12). Subsequent studies revealed that this antagonistic relationship may result in human cancers with specific defects in BAF subunits to become dependent on the activity of the polycomb repressive group 2 (PRC2) complex. This is best exemplified in MRTs, as loss of SNF5 results in the altered genomic occupancy of the repressive chromatin mark deposited by PRC2 at histone H3 lysine 27 residues (H3K27me3), leading to the repression of lineage-specific targets (13). In these models, disruption of the histone methyltransferase activity of EZH2, the catalytic subunit of PRC2, impaired tumor growth, thereby demonstrating that SNF5 mutant tumors depend on EZH2 activity (13, 14). More recently, a similar dependency on EZH2 was described in the context of ARID1A mutant cancers, suggesting that PRC2 activity may be a common vulnerability in SWI/SNF-defective lesions (15). However, whether targeting EZH2 will be effective in all cancers harboring these specific mutations or in other SWI/SNF subunit mutant contexts remains an open question.

Significance

Targeting epigenetic dependencies caused by mutations in chromatin-modifying enzymes represents a novel therapeutic approach in cancer. Notably, cancers harboring mutations in the SNF5 subunit of the SWI/SNF chromatin remodeling complex have been shown to be susceptible to small-molecule inhibitors of the EZH2 histone methyltransferase that are currently in clinical development. We demonstrate that EZH2 inhibition can be effective in SMARCA4 mutant cancers that concurrently transcriptionally silence the paralog helicase SMARCA2. SMARCA2 is directly suppressed by EZH2, and SMARCA2 expression levels predict EZH2 inhibitor activity in other SWI/SNF mutant contexts, including ARID1A mutant tumors. These data provide insight into the utility of EZH2 inhibitors in SWI/SNF mutant tumors and have important implications regarding predictive diagnostics.

Author contributions: T.J., X.Y., R.B., S.G., and R.L.Y. designed research; T.J., X.Y., B.A., T.S., B.H., Z.M., S.G., and R.L.Y. performed research; T.J., X.Y., R.B., B.A., T.S., and R.L.Y. analyzed data; and R.L.Y. wrote the paper.

The authors declare no conflict of interest.

This article is a PNAS Direct Submission.

[1]T.J and X.Y. contributed equally to this work.

[2]To whom correspondence should be addressed. Email: yauch.bob@gene.com.

This article contains supporting information online at www.pnas.org/lookup/suppl/doi:10.1073/pnas.1703966114/-/DCSupplemental.

Multiple inhibitors targeting the enzymatic activity of EZH2 are currently in clinical development, with EPZ-6438 (tazemontstat) representing the most clinically advanced molecule. Early clinical data presented with EPZ-6438 has shown promise, as objective responses have been observed in a subset of SNF5 mutant and SMARCA4 mutant patients treated with EPZ-6438 as a single agent. These data not only begin to provide early clinical proof of concept, but indicate that EZH2 inhibition may be effective in the context of SMARCA4 mutant cancers, a preclinical finding that has yet to be published. Notably, not all patients with tumors harboring SNF5 or SMARCA4 defects responded to therapy, suggesting that identifying a biomarker predictive of response to EZH2 inhibition could provide significant benefit. In the present study, we demonstrate that EZH2 inhibition is effective in a subset of SMARCA4 mutant cancer models, and that the PRC2-mediated transcriptional suppression of the paralog ATPase, SMARCA2, can predict the preclinical activity of EZH2 inhibitors. Importantly, we show that the level of SMARCA2 expression may be a global predictive biomarker of EZH2 activity in other BAF mutant cancers.

Results

A Subset of SMARCA4 Mutant Cancers Is Responsive to EZH2 Inhibition. We evaluated the effect of EZH2 inhibition using the EZH2-targeting histone methyltransferase inhibitor, EPZ-6438, on clonogenic growth across a panel of 11 *SMARCA4* mutated cancer cell lines derived from different tumor types (Dataset S1). A dose-dependent inhibition of clonogenic growth independent of tissue derivation was observed in a subset of these *SMARCA4* mutant cell lines (Fig. 1*A*). The degree of growth inhibition on EPZ-6438 treatment was similar to that previously described in models characterized by mutations in *SNF5* (G401). No activity was observed in a panel of SWI/SNF wild-type models ($n = 8$). The differential sensitivity to EPZ-6438 was not due to differences in target engagement, as a similar dose-dependent inhibition of H3K27 methylation was observed in sensitive and resistant models (*SI Appendix*, Fig. S1). Furthermore, differences in global levels of H3K27 methylation or expression levels of the PRC2 components, EZH2 and SUZ12, did not underlie the differential sensitivity to EPZ-6438 (*SI Appendix*, Fig. S2). The dose-dependent inhibition in colony formation was phenocopied using two additional EZH2 methyltransferase inhibitors, GSK-126 and CPI-169 (*SI Appendix*, Fig. S3). Furthermore, genetic ablation of EZH2 through CRISPR-mediated gene editing resulted in an inhibition of colony formation in *SMARCA4* mutant TOV-112D cells, which were sensitive to EPZ-6438, but had no effect on colony formation in EPZ-6438–resistant *SMARCA4* mutant cells (H1299 and A549) (*SI Appendix*, Fig. S4). Taken together, these data strongly suggest that the differential effect of EPZ-6438 on colony formation in SMARCA4 mutant cells is dependent on EZH2.

EZH2 inhibition led to a heterogenous phenotypic response in cells. In contrast to resistant models, EPZ-6438–sensitive models consistently acquired pronounced morphological changes after 7 d of treatment, characterized by cell flattening and enlargement (*SI Appendix*, Fig. S5*A*). A strong apoptotic response was observed in the TOV-112D model following 7 d of EPZ-6438 treatment, whereas several other models showed evidence of subpopulations of apoptotic cells following prolonged exposure with EPZ-6438 (Fig. 1*B* and *SI Appendix*, Fig. S5*B*). Increases in senescence-associated β-galactosidase expression were observed in some SMARCA4 mutant EPZ-6438–sensitive models. This was most notable in the COV434 and NCI-H522 cell lines that lacked evidence of apoptosis (Fig. 1*C*); however, subpopulations of β-galactosidase–positive cells were also noted in cell lines that exhibited evidence for apoptosis at later time points (e.g., NCI-H661 cells). Finally, the kinetics of senescence induction varied, with the COV434 model exhibiting homogenous expression of β-galactosidase by 7 d of treatment with EPZ-6438, whereas homogenous β-galactosidase expression was not observed until a few weeks of EPZ-6438 treatment in NCI-H522 cells, even though these cells remained in a nonproliferative state based on Edu incorporation (*SI Appendix*, Fig. S5*C*). Treatment of SCID mice bearing NCI-H522 cells grown as xenografts

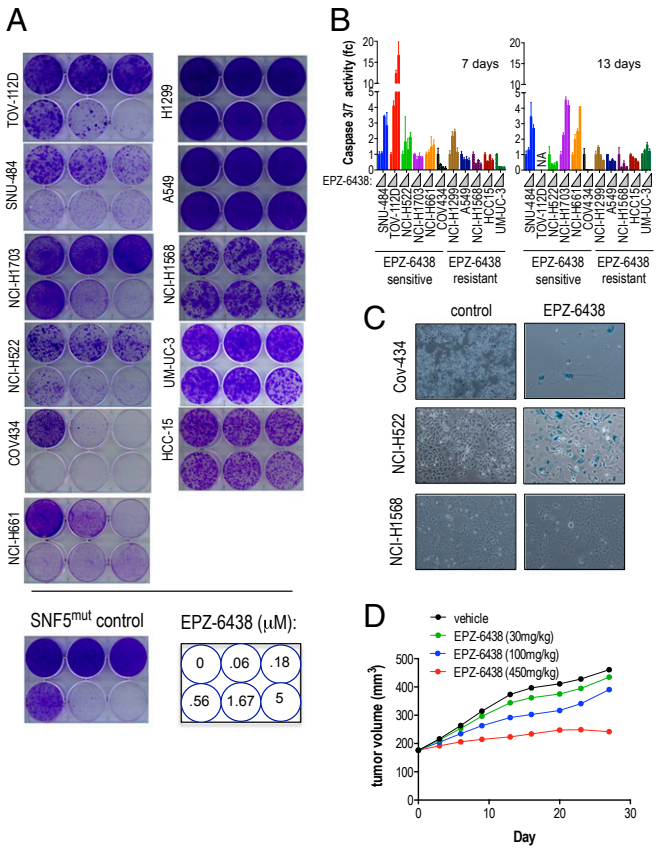

Fig. 1. EZH2 inhibition suppresses growth in a subset of SMARCA4 mutant cancers. (*A*) Effect of treatment with various doses of EPZ-6438 on clonogenic growth across a panel of SMARCA4 mutant cancer cell lines. SNF5 mutant G401 cells served as a positive control. The dosing scheme is shown. (*B*) Caspase 3/7 activation on treatment of cell lines with various doses of EPZ-6438 (0, 0.74, 2.2, and 6.7 μM) following 7 d (*Left*) and 13 d (*Right*) of treatment. Data are presented as an average fc in caspase 3/7 fluorescent counts relative to DMSO control across triplicate samples. Error bars represent SD. (*C*) Staining of β-galactosidase in representative SMARCA4 mutant models. (*D*) Dose-dependent inhibition of in vivo growth of NCI-H522 xenografts following twice-daily oral administration of EPZ-6438 treatment for 23 d. Data are presented as cubic regression splines of tumor volumes over time plotted on the natural scale.

resulted in a dose-dependent inhibition of tumor growth following twice daily (b.i.d.) administration of EPZ-6438 (Fig. 1*D*), with the strongest tumor growth inhibition (72%) and reductions in H3K27me3 and H3K27me2 observed at the 450 mg/kg b.i.d. dose (*SI Appendix*, Fig. S6).

SMARCA2 Expression Associates with Differential Sensitivity to EZH2 Inhibition in SMARCA4-Mutant Cancer Models. To elucidate differences underlying EPZ-6438 sensitivity, we carried out gene expression profiling across these 11 SMARCA4 mutant models. A supervised analysis of the most differentially expressed genes revealed that EPZ-6438–sensitive models exhibited a greater number of commonly repressed genes (Fig. 2*A* and Dataset S2). Genes with significantly reduced expression levels across EPZ-6438–sensitive cell lines were enriched for a set of genes previously observed to be up-regulated following EZH2 knockdown (MSigDB:M4196, 12/50; $P = 1.5e10^{-5}$, Fisher's exact test; Dataset S3) (16). Among these, we observed that expression levels of the paralog SWI/SNF helicase *SMARCA2* were reduced in all SMARCA4 mutant models that were sensitive to EZH2 inhibition. This association was confirmed at the transcript level by quantitative RT-PCR (*SI Appendix*, Fig. S7) and at the protein level by Western blot analysis (Fig. 2*B*).

All other SWI/SNF complex components were expressed to an equal extent across the EPZ-6438–sensitive and –resistant models (*SI Appendix*, Fig. S8). We did not detect any underlying genomic abnormalities (e.g., copy number loss, mutation) that could result in a loss of SMARCA2 in these models.

Because SMARCA2 has been previously identified as epigenetically regulated in specific contexts, we evaluated whether *SMARCA2* could be under PRC2-mediated suppression (17). Treatment with EPZ-6438 resulted in a significant up-regulation of *SMARCA2* transcript specifically in EPZ-6438–sensitive, but not –resistant, cell lines (Fig. 2*C*), suggesting that PRC2 activity contributes to transcriptional regulation of SMARCA2 in these models. To clarify this, we performed a ChIP-seq experiment using representative EPZ-6438–sensitive and –resistant cell lines, and observed strong and specific enrichment of H3K27me3 around the *SMARCA2* transcriptional start site only in the sensitive cell line (*SI Appendix*, Fig. S9). We were then able to confirm this trend across the full panel of SMARCA4 mutant cell lines by performing H3K27me3 ChIP and assessing associations of the H3K27me3 mark at three targeted locations within the *SMARCA2* promoter via PCR (Fig. 2*D*). A similar enrichment of EZH2 was observed at the *SMARCA2* promoter in sensitive cell lines, and treatment of sensitive cells with EPZ-6438 resulted in the depletion of H3K27me3 from the *SMARCA2* promoter (*SI Appendix*, Fig. S10). Furthermore, the kinetics of SMARCA2 induction on treatment with EPZ-6438 were similar to those of other previously described H3K27me3-enriched PRC targets (*SI Appendix*, Fig. S10). Taken together, these data indicate that *SMARCA2* is under direct PRC2-mediated suppression in cell lines sensitive to EZH2 inhibition.

The SWI/SNF helicases SMARCA4 and SMARCA2 have been shown to have either redundant or nonredundant functionalities, depending on the cellular context (18–20). To address whether SMARCA2 could compensate for the transcriptional effects of SMARCA4 in this cellular context, we engineered TOV-112D cells to express either a doxycycline (dox)-inducible SMARCA2 or SMARCA4 construct. Dox treatment of these cells resulted in the induction of SMARCA2 or SMARCA4 protein localizing to the insoluble nuclear fraction and reassociating with the core SWI/SNF complex protein, SMARCC1 (*SI Appendix*, Fig. S11). Analysis of gene expression changes following the dox-induced expression of SMARCA2 and SMARCA4 revealed a statistically significant ($P <$ 2e-16, Fisher's exact test) overlap in genes regulated by these helicases (Fig. 3*A*). As expected, the induction of SMARCA2 and SMARCA4 resulted in primarily the up-regulation of gene expression, with >70% of the most strongly induced genes [log2 fold change (fc) ≥2] shared between SMARCA2 and SMARCA4. Furthermore, these genes significantly ($P <$ 2e-16, Fisher's exact test) overlapped with those derepressed on EZH2 inhibitor treatment (Fig. 3*B* and Dataset S4), demonstrating that SMARCA2 and/or SMARCA4 can regulate a large subset of the genes that are repressed by PRC2. Gene set enrichment analysis revealed that genes associated with extracellular matrix and cell migration/motility were more strongly enriched among the EZH2-regulated genes that are antagonized by SMARCA2/A4 compared with those EZH2-regulated genes that are unresponsive to SMARCA2/A4 (Fig. 3*C*, *SI Appendix*, Fig. S12, and Datasets S5–S8).

Induction of SMARCA2 on EZH2 Inhibition Is Required for Apoptosis in TOV-112D Cells. To determine whether the derepression of SMARCA2 on EPZ-6438 treatment is required to inhibit clonogenic growth, we engineered cells to express a stable shRNA targeting *SMARCA2* (shSMARCA2) before treatment with EPZ-6438. Preventing the induction of SMARCA2 on EZH2 inhibition did not impact the antiproliferative effect of EPZ-6438 in three of the four SMARCA4 mutant cell lines tested (*SI Appendix*, Fig. S13), but significantly diminished the effect of EZH2 inhibition on clonogenic growth in TOV-112D cells (Fig. 4*A*). Expression of shSMARCA2 did not impact the EPZ-6438–mediated inhibition of H3K27 methylation in TOV-112D cells, but did block the induction of SMARCA2 after drug treatment (*SI Appendix*, Fig. S14). Because we had previously observed the strongest apoptotic response to EPZ-6438 treatment in TOV-112D cells, we evaluated whether shSMARCA2 could specifically impact apoptosis induction in this model by monitoring caspase 3/7 activity. Expression of shSMARCA2, but not of a nontargeting control shRNA (shNTC), inhibited the dose-dependent activation of caspase 3/7 in TOV-

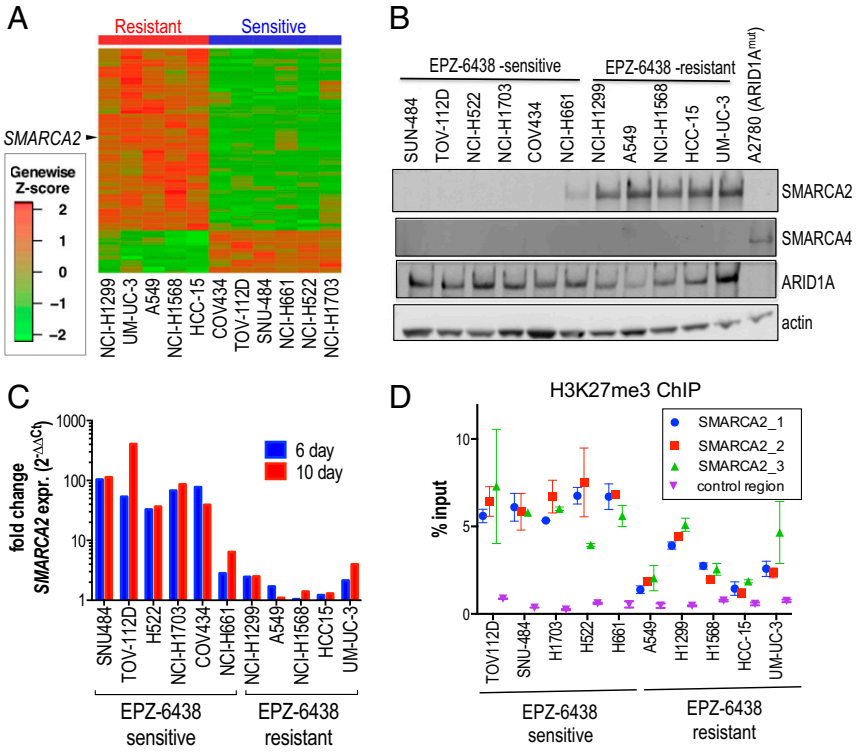

Fig. 2. SMARCA2 expression level is associated with differential sensitivity to EZH2 inhibition in SMARCA4 mutant cancer models. (*A*) Supervised analysis of genes most differentially expressed (log-2 fc >1; $P \leq 0.05$) between EPZ-6438–sensitive ($n = 6$) and –resistant ($n = 5$) SMARCA4 mutant models. Expression estimates are reported as *z*-scores derived from log2 reads per kilobase per million mapped reads. (*B*) Western blot analysis of SMARCA2 levels across SMARCA4 mutant models showing differential expression between EPZ-6438–sensitive and –resistant models. A2780 cells served as SMARCA4 wild-type control. (*C*) Quantitative PCR analysis of *SMARCA2* transcript levels in SMARCA4 mutant cells treated with 5 μM of EPZ-6438 for 6 or 10 d demonstrating selective induction of *SMARCA2* mRNA in EPZ-6438–sensitive models. Relative gene expression was calculated with the $2^{-\Delta\Delta Ct}$ method, using *GUSB* as a reference gene and mock (DMSO) treatment as the calibrator. (*D*) Quantitative PCR analysis of H3K27me3 ChIP DNA enrichment at three locations in the SMARCA2 gene promoter (chr9:2015841–2015938, blue; chr9:2016847–2016917, red; chr9:2016214–2016333, green markers) and a control region (actin promoter, purple marker) across SMARCA4 mutant cancer cell lines. The *y*-axis indicates average enrichment of the region in the H3K27me3 IP as a percentage of the level observed in the input lysate. Error bars indicate SD of the mean estimated from two independent IPs.

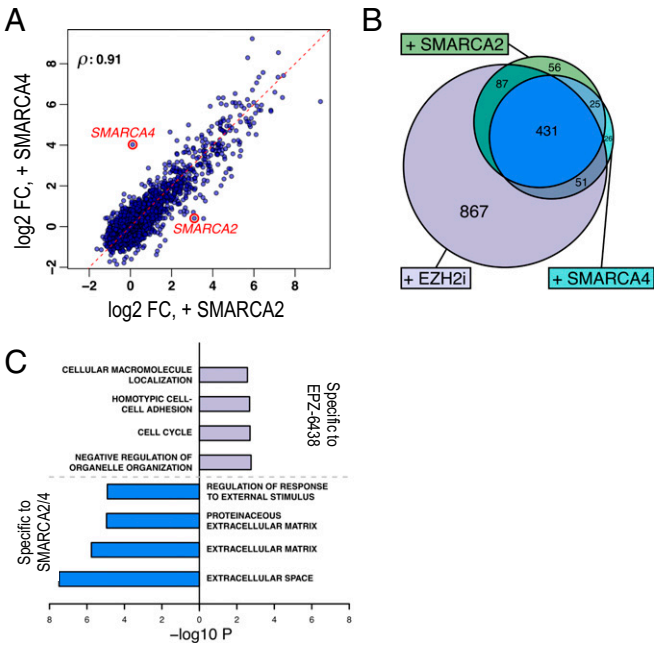

Fig. 3. Overlap in gene expression changes on SMARCA2 or SMARCA4 induction. (*A*) Scatterplot depicting log2 fc expression estimates for all genes following dox-inducible expression of SMARCA2 (*x*-axis) and SMARCA4 (*y*-axis) in TOV-112D cells. The sets of genes significantly differentially expressed following induction of either helicase significantly overlap ($P < 2e\text{-}16$, Fisher's exact test). Genes nonspecifically impacted by dox treatment in vector control TOV-112D cells were filtered from this analysis. (*B*) Venn diagram depicting the overlap between genes significantly differentially expressed (log2 fc >1; $P < 0.05$) following dox-induced expression of SMARCA4 or SMARCA2, or treatment with 1 μM of EPZ-6438 (+EZH2i) in TOV-112D cells. (*C*) Gene Ontology annotations disproportionately enriched among EPZ-6438–induced genes within the subset regulated by SMARCA2/A4 vs. those unresponsive to SMARCA2/A4 (specific to EPZ-6438).

112D cells (Fig. 4*B*). This finding was further confirmed in TOV-112D clones engineered to ablate the SMARCA2 gene by CRISPR-mediated genome editing (*SI Appendix*, Fig. S15).

To begin to elucidate the mechanism(s) by which the EPZ-6438–mediated derepression of SMARCA2 contribute(s) to apoptosis, we evaluated gene expression changes regulated by EZH2 inhibition in the presence or absence of shSMARCA2 expression, as well as in SMARCA2 KO clones. As expected, EZH2 inhibition resulted in a strong up-regulation of gene expression in control cells; however, blocking the induction of SMARCA2 had little effect on the overall number or magnitude of EPZ-6438–regulated genes globally (Fig. 4*C*, *SI Appendix*, Fig. S16, and Dataset S9). We did identify a small number of genes ($n = 9$) that were specifically impacted by both shSMARCA2 and *SMARCA2* gene ablation (Fig. 4*D* and Dataset S9; Q value < 0.05); including cathepsin B (*CTSB*), a lysosomal cysteine protease specifically linked to apoptotic cell death in certain cellular contexts (21, 22). CTSB transcript and protein were strongly up-regulated in control cells on EZH2 inhibition; however, this up-regulation was blocked by targeting SMARCA2 (Fig. 4 *D* and *E*). To determine whether CTSB can contribute to apoptosis in response to EZH2 inhibition in TOV-112D cells, we similarly expressed three separate shRNAs targeting CTSB in cells. Expression of shCTSB significantly suppressed the activation of caspase 3/7 in response to EPZ-6438 (Fig. 4*F*). As opposed to blocking the induction of SMARCA2 directly, blocking CTSB induction did not completely abrogate caspase 3/7 activation. These data suggest that CTSB contributes to apoptosis in response to EZH2 inhibition, but is not fully sufficient for mediating apoptosis.

The Association of SMARCA2 Expression with Sensitivity to EZH2 Inhibition Extends to Other SWI/SNF Mutant Contexts. To determine whether the association between SMARCA2 expression levels and EZH2 inhibitor activity extends to other BAF complex mutations, we similarly evaluated the effect of EPZ-6438 on clonogenic growth across a panel of SNF5 mutant ($n = 2$) and ARID1A mutant ($n = 7$) cancer cell lines (Dataset S1). Dose-dependent inhibition of clonogenic growth was observed in both SNF5 mutant cell lines, but in only a subset of the ARID1A mutant cancer cell lines (Fig. 5*A*). Growth inhibition was dependent on EZH2, as genetic ablation of EZH2 inhibited clonogenic growth in the EPZ-6438–sensitive model; however, TOV-21G had no effect on colony formation in the EPZ-6438–resistant ARID1A mutant model, OVISE, or in control models harboring no known mutations in any SWI/SNF complex members (*SI Appendix*, Fig. S17). The differential sensitivity to

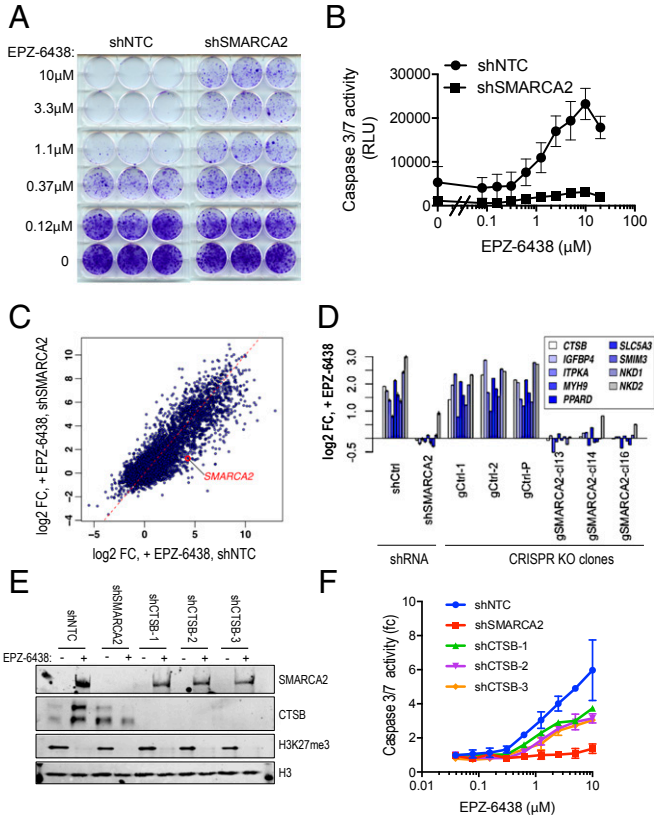

Fig. 4. Induction of SMARCA2 on EZH2 inhibition is required for apoptosis through a mechanism involving CTSB. (*A*) Stable expression of a shRNA targeting SMARCA2 can suppress the EPZ-6438–induced inhibition of clonogenic growth in TOV-112D cells, in contrast to shNTC. (*B*) Expression of a SMARCA2 shRNA abrogates the activation of caspase 3/7 (Caspase Glo Assay) on EPZ-6438 treatment, demonstrating that the derepression of SMARCA2 is required for apoptosis. Mean values across triplicate cultures were measured. Error bars represent SD. (*C*) Scatterplot depicting the log2 fc in estimated expression for all genes following treatment with 5 μM of EPZ-6438 in TOV-112D cells that express a nontargeting shRNA (*x*-axis) or a SMARCA2-targeting shRNA (*y*-axis). Estimates are derived from three independent treatments per cell line. (*D*) Changes in expression level of genes identified as significantly regulated on treatment with 5 μM of EPZ-6438 in control TOV-112D cells (shNTC or control KO clones), but not significantly regulated by EPZ-6438 on expression of shSMARCA2 and in clones engineered to genetically ablate SMARCA2 expression through CRISPR. (*E*) Western blot analysis of TOV112D cells expressing an shRNA targeting SMARCA2 or three separate shRNAs targeting CTSB on expression of SMARCA2 and CTSB following treatment with EPZ-6438. H3K27me3 served as a control for the EPZ-6438 treatment. (*F*) Expression of shRNAs targeting CTSB can significantly suppress the activation of caspase 3/7 on treatment with EPZ-6438.

EZH2 inhibition was also phenocopied using another EZH2 inhibitor (CPI-169; *SI Appendix*, Fig. S18) and phenocopied when ARID1A mutant cells were grown in 3D cultures using Matrigel (*SI Appendix*, Fig. S19). The observed in vitro activity further translated to in vivo efficacy, as treatment of SCID mice bearing TOV-21G tumor xenografts resulted in tumor growth inhibition at the 450 mg/kg b.i.d. dose (Fig. 5*B* and *SI Appendix*, Fig. S20). Analysis of constitutive *SMARCA2* transcript levels revealed that *SMARCA2* was repressed in the *SNF5* mutant and *ARID1A* mutant cancer cell lines that were sensitive to EPZ-6438 treatment relative to the drug-resistant ARID1A mutant or wild-type lines examined (Fig. 5*C*, *Left*). Overall, there was a statistically significant ($P < 0.001$) association of *SMARCA2* expression levels and sensitivity to EPZ-6438 in all models tested (Fig. 5*C*, *Right*). Finally, similar to observations in the SMARCA4 mutant models, treatment of EPZ-6438–sensitive SNF5 mutant or ARID1A mutant models with EPZ-6438 resulted in induction of *SMARCA2* transcript, which was not regulated in resistant models (Fig. 5*D*).

Discussion

Our study provides several insights into targeting EZH2 as a therapeutic approach in cancers harboring defects in the SWI/SNF chromatin remodeling complex. First, the data are supportive of a dependency on EZH2 in a subset of, but not all, SWI/SNF mutant cancers, including SMARCA4 mutant cancers, which has yet to be reported. This difference is not due to an inability of EZH2 inhibitors to suppress enzymatic activity in resistant models, as H3K27me3 levels were equally reduced. Neither is it due to potential off-target properties of EPZ-6438 specifically, as the variable antiproliferative effects were consistently phenocopied using two additional EZH2 inhibitors, GSK-126 and CPI-169 (23, 24). An identical sensitivity pattern was likewise observed when ARID1A mutant ovarian cells were grown as acini in 3D, suggesting that the differences in sensitivity are not driven by the specific cell culture conditions used to assay the drug's effect (15). Finally, in contrast to previous reports, we did not observe any evidence of a noncatalytic function for EZH2 in SMARCA4 or ARID1A mutant cancer cell lines that were resistant to the methyltransferase inhibitor, as genetic ablation of EZH2 in these cells did not impact growth/survival (25). EZH2 knockout did suppress growth in cells sensitive to the enzymatic inhibitor. Taken together, these data strongly support that only a subset of SWI/SNF mutant models may be dependent on EZH2.

Second, we found that the expression level of the ATPase SMARCA2 is a predictive biomarker for the antiproliferative effects of EZH2 inhibition across multiple BAF mutant cancer models. It was previously recognized that SMARCA2 is inactivated through an undefined epigenetic mechanism in a subset of cancers harboring mutations in BAF complex components (17, 26). Here we demonstrated that PRC2 is directly responsible for this epigenetic suppression of SMARCA2, as the SMARCA2 promoter is occupied by H3K27me3 marks in sensitive cell lines with low SMARCA2 expression levels, and EZH2 inhibition can deplete these marks to restore SMARCA2 expression. Despite the strong association of PRC2-mediated SMARCA2 repression with sensitivity to EZH2 inhibitors, the functional significance of SMARCA2 repression in these models remains incompletely understood. It is possible that the PRC2-mediated inactivation of SMARCA2 may serve as a mechanism to help maintain maximal repression of PRC2 targets. Consistent with this, we have demonstrated that SMARCA2 expression can antagonize a large set of PRC2 targets in SMARCA4 mutant cells. These targets overlap with those induced on reintroduction of SMARCA4, supporting a functional redundancy in this context. However, the relationship is less clear in the context of SNF5 or ARID1A mutant tumors that are dependent on PRC2, because these tumors still express residual SMARCA4-containing complexes that are devoid of SNF5 or ARID1A (27). Furthermore, contradictory data exist regarding the requirement for SMARCA2 expression in mediating growth inhibition in models characterized by silenced SMARCA2. For

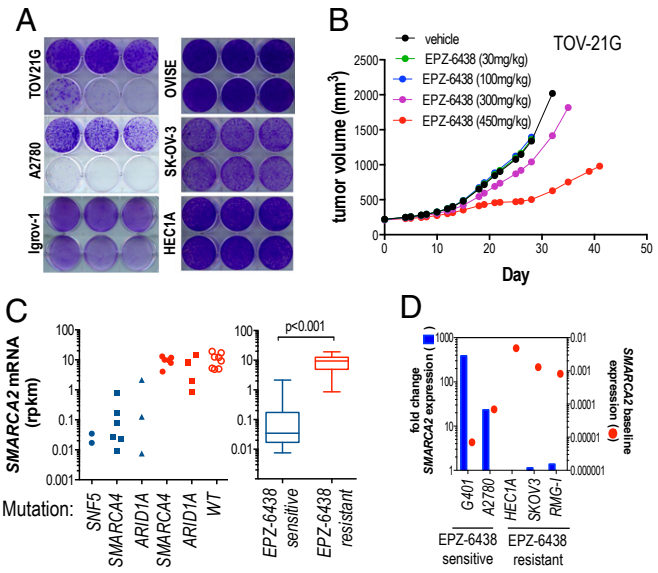

Fig. 5. SMARCA2 expression levels are associated with differential sensitivity to EZH2 inhibition in additional SWI/SNF mutant contexts. (*A*) Effect of treatment with various doses of EPZ-6438 on clonogenic growth across a panel of ARID1A mutant cancer cell lines, a subset of which are sensitive to EPZ-6438. The dosing scheme is identical to that presented in Fig. 1*A*. (*B*) In vivo tumor growth following twice-daily administration of the indicated doses of EPZ-6438 for 28 d in TOV-21G xenografts. Data are presented as cubic regression splines of tumor volumes over time plotted on the natural scale. (*C*) Expression of SMARCA2 mRNA levels between cell lines defined as sensitive (blue symbols) or resistant (red symbols) to EPZ-6438, based on inhibition of clonogenic growth. Models include SNF5 mutant ($n = 2$), SMARCA4 mutant ($n = 11$), ARID1A mutant ($n = 7$), and SWI/SNF wild-type (wt; $n = 8$) cell lines, indicated on the *x*-axis. The graph to the right shows a clear association between SMARCA2 expression levels and sensitivity to EPZ-6438 when all tested models were considered together. Significance was estimated using the Mann–Whitney *U* test. (*D*) Quantitative PCR analysis of *SMARCA2* transcript levels in SNF5 mutant (G401), ARID1A mutant (A2780, HEC1A, and SKOV3), and wild-type (RMG-I) cells treated with 5 μM of EPZ-6438 demonstrating selective induction of *SMARCA2* mRNA in EPZ-6438–sensitive models. The fc in *SMARCA2* mRNA expression on EPZ-6438 treatment relative to DMSO control is depicted by bars (left *y*-axis). The right *y*-axis indicates the baseline expression level of *SMARCA2* ($2^{-\Delta Ct}$) relative to the control gene, *GUSB*.

instance, it has been reported that reintroduction of SMARCA2 directly into SMARCA4/A2-deficient cells results in growth arrest (28, 29). However, taking an alternative approach that alleviates the potential for mislocalization of ectopically expressed SMARCA2, we demonstrated that the derepression of SMARCA2 was not required for the antiproliferative effects on EZH2 inhibition in several models tested. At the same time, restoration of SMARCA2 expression was required to drive apoptosis in a SMARCA4 mutant model that was highly sensitive to EZH2 inhibition. In this case, the SMARCA2-mediated induction of CTSB, a cysteine protease that can drive cells toward programmed cell death in specific contexts, contributed to apoptosis on EZH2 inhibition (21, 22). However, blocking the EPZ-6438-mediated induction of CTSB did not fully abrogate apoptosis, suggesting that other SMARCA2-dependent genes may be involved. Taken together, the data support a strong association of SMARCA2 loss in BAF mutant cancers and PRC2 dependency, but the functional implications of SMARCA2 repression remain less clear.

Given the role of PRC2 in lineage specification and maintenance, the PRC2 dependency observed in the subset of BAF mutant cancers could be an indicator of the lineage and/or progenitor state from which these cancers originated (30). In support of this idea, nearly all SMARCA4 mutant SCCOHTs and a high percentage of SNF5 mutant MRTs exhibit the concurrent loss of

SMARCA2 (29, 31, 32). Despite different tissues of origin, these tumors often share many molecular and clinicopathological features and have been proposed to represent a similar class of rhabdoid-like cancers (33). The situation is more complicated in the context of SMARCA4 mutant lung cancers, as SMARCA2 loss represents a much smaller percentage of these cancers, and those that are proficient in SMARCA2 require the residual SMARCA2-containing BAF complexes for survival (20, 34–36). However, recent studies have identified a group of undefined thoracic malignancies harboring SMARCA4 mutations that are distinct from SMARCA4 mutant lung carcinomas but related to SCCOHTs and MRTs (37). These newly defined SMARCA4-deficient thoracic sarcomas (DTSs) exhibit decreased SMARCA2 levels compared with lung carcinomas with SMARCA4 mutations and can be differentiated from SMARCA4 mutant lung carcinomas based on SOX2 expression levels. Although the lung cancer models used in this study do not necessarily represent DTSs, it is interesting to note that all three of the EPZ-6438–sensitive lung models exhibited elevated SOX2 expression relative to the EPZ-6438–resistant lung cancer cell lines, even though they were derived from patients with adenocarcinoma (NCI-H522), large-cell carcinoma (NCI-H661), or squamous cell carcinoma (NCI-H1703) (*SI Appendix*, Fig. S21). Given that we can now differentiate SWI-SNF mutant tumors that are dependent on PRC2 based on SMARCA2 expression within a given tissue type, a more careful examination will be needed to determine whether they exhibit distinct morphological and/or molecular features possibly indicative of a different cellular origin.

Finally, our findings have important implications for the development of predictive diagnostics for the various inhibitors of EZH2 that are under clinical development. Current clinical development strategies have focused on evaluating EZH2 inhibitors in the context of specific tumor types with known BAF mutations (ClinicalTrials.gov, identifiers NCT02601950 and NCT02601937). The data presented here strongly suggest that a diagnostic test based on evaluating SMARCA2 levels in patient tumors could better focus these trials on patients who are likely to respond positively to EZH2 inhibition.

Materials and Methods

In Vitro Assays. Clonogenic assays were carried out by culturing cells in six-well plates with DMSO or the indicated concentrations of drug until DMSO-treated cultures reached confluence (typically ∼14–24 d). Colonies were visualized by staining with 0.5% crystal violet. Apoptosis was monitored through either live cell imaging using the Incucyte Caspase 3/7 Apoptosis Assay (Essen Biosciences) or through a static time point assessment using the Caspase-Glo 3/7 Assay (Promega), in accordance with the manufacturer's instructions. Senescence was monitored by staining for β-galactosidase activity using the Sigma-Aldrich Senescence Cell Histochemical Staining Kit. Detailed descriptions of the methodologies are provided in *SI Appendix, Materials and Methods*.

Quantitative RT-PCR. Cells were treated with medium containing 5 μM of EPZ-6438 for 6 or 10 d, with fresh medium replaced every 3–4 d. *SMARCA2* gene expression levels were determined by the Taqman gene expression assay (Hs01030846_m1; Thermo Fisher Scientific). Expression levels were calculated by the $2^{-\Delta\Delta Ct}$ method, using *GUSB* as a reference gene and mock (DMSO) treatment as the calibrator in experiments involving EPZ-6438 treatment.

Xenograft Studies. All in vivo studies were conducted in compliance with Genentech's Institutional Animal Care and Use Committee. Mice bearing established tumors were separated into groups with equal-sized tumors to receive escalating doses of EPZ-6438. Tumor volumes were calculated based on perpendicular length and width caliper measurements using the following formula: tumor volume (mm^3) = 0.5 × (length × $width^2$). A mixed modeling approach was used to analyze the repeat measurements of tumor volumes. The methodology and analysis are described in detail in *SI Appendix, Materials and Methods*.

Detailed information on reagents, as well as on the analysis of RNA-seq, ChIP-seq, and ChIP-PCR datasets, is provided in *SI Appendix, Materials and Methods*.

1. Kadoch C, Crabtree GR (2015) Mammalian SWI/SNF chromatin remodeling complexes and cancer: Mechanistic insights gained from human genomics. *Sci Adv* 1:e1500447.
2. Masliah-Planchon J, Bièche I, Guinebretière J-M, Bourdeaut F, Delattre O (2015) SWI/SNF chromatin remodeling and human malignancies. *Annu Rev Pathol* 10:145–171.
3. Biegel JA, Busse TM, Weissman BE (2014) SWI/SNF chromatin remodeling complexes and cancer. *Am J Med Genet C Semin Med Genet* 166C:350–366.
4. Versteege I, et al. (1998) Truncating mutations of hSNF5/INI1 in aggressive paediatric cancer. *Nature* 394:203–206.
5. Roberts CW, Galusha SA, McMenamin ME, Fletcher CD, Orkin SH (2000) Haploinsufficiency of Snf5 (integrase interactor 1) predisposes to malignant rhabdoid tumors in mice. *Proc Natl Acad Sci USA* 97:13796–13800.
6. Guidi CJ, et al. (2001) Disruption of Ini1 leads to peri-implantation lethality and tumorigenesis in mice. *Mol Cell Biol* 21:3598–3603.
7. Wu JN, Roberts CWM (2013) ARID1A mutations in cancer: Another epigenetic tumor suppressor? *Cancer Discov* 3:35–43.
8. Jelinic P, et al. (2014) Recurrent SMARCA4 mutations in small cell carcinoma of the ovary. *Nat Genet* 46:424–426.
9. Witkowski L, et al. (2014) Germline and somatic SMARCA4 mutations characterize small cell carcinoma of the ovary, hypercalcemic type. *Nat Genet* 46:438–443.
10. Mathur R, et al. (2017) ARID1A loss impairs enhancer-mediated gene regulation and drives colon cancer in mice. *Nat Genet* 49:296–302.
11. Glaros S, Cirrincione GM, Palanca A, Metzger D, Reisman D (2008) Targeted knockout of BRG1 potentiates lung cancer development. *Cancer Res* 68:3689–3696.
12. Kadoch C, Copeland RA, Keilhack H (2016) PRC2 and SWI/SNF chromatin remodeling complexes in health and disease. *Biochemistry* 55:1600–1614.
13. Wilson BG, et al. (2010) Epigenetic antagonism between polycomb and SWI/SNF complexes during oncogenic transformation. *Cancer Cell* 18:316–328.
14. Knutson SK, et al. (2013) Durable tumor regression in genetically altered malignant rhabdoid tumors by inhibition of methyltransferase EZH2. *Proc Natl Acad Sci USA* 110:7922–7927.
15. Bitler BG, et al. (2015) Synthetic lethality by targeting EZH2 methyltransferase activity in ARID1A-mutated cancers. *Nat Med* 21:231–238.
16. Nuytten M, et al. (2008) The transcriptional repressor NIPP1 is an essential player in EZH2-mediated gene silencing. *Oncogene* 27:1449–1460.
17. Glaros S, et al. (2007) The reversible epigenetic silencing of BRM: Implications for clinical targeted therapy. *Oncogene* 26:7058–7066.
18. Kadam S, Emerson BM (2003) Transcriptional specificity of human SWI/SNF BRG1 and BRM chromatin remodeling complexes. *Mol Cell* 11:377–389.
19. Flowers S, Nagl NG, Jr, Beck GR, Jr, Moran E (2009) Antagonistic roles for BRM and BRG1 SWI/SNF complexes in differentiation. *J Biol Chem* 284:10067–10075.
20. Hoffman GR, et al. (2014) Functional epigenetics approach identifies BRM/SMARCA2 as a critical synthetic lethal target in BRG1-deficient cancers. *Proc Natl Acad Sci USA* 111:3128–3133.
21. Foghsgaard L, et al. (2001) Cathepsin B acts as a dominant execution protease in tumor cell apoptosis induced by tumor necrosis factor. *J Cell Biol* 153:999–1010.
22. de Castro MAG, Bunt G, Wouters FS (2016) Cathepsin B launches an apoptotic exit effort upon cell death-associated disruption of lysosomes. *Cell Death Dis* 2:16012.
23. McCabe MT, et al. (2012) EZH2 inhibition as a therapeutic strategy for lymphoma with EZH2-activating mutations. *Nature* 492:108–112.
24. Bradley WD, et al. (2014) EZH2 inhibitor efficacy in non-Hodgkin's lymphoma does not require suppression of H3K27 monomethylation. *Chem Biol* 21:1463–1475.
25. Kim KH, et al. (2015) SWI/SNF-mutant cancers depend on catalytic and non-catalytic activity of EZH2. *Nat Med* 21:1491–1496.
26. Gramling S, Rogers C, Liu G, Reisman D (2011) Pharmacologic reversal of epigenetic silencing of the anticancer protein BRM: A novel targeted treatment strategy. *Oncogene* 30:3289–3294.
27. Wang X, et al. (2009) Oncogenesis caused by loss of the SNF5 tumor suppressor is dependent on activity of BRG1, the ATPase of the SWI/SNF chromatin remodeling complex. *Cancer Res* 69:8094–8101.
28. Strober BE, Dunaief JL, Guha, Goff SP (1996) Functional interactions between the hBRM/hBRG1 transcriptional activators and the pRB family of proteins. *Mol Cell Biol* 16:1576–1583.
29. Karnezis AN, et al. (2016) Dual loss of the SWI/SNF complex ATPases SMARCA4/BRG1 and SMARCA2/BRM is highly sensitive and specific for small cell carcinoma of the ovary, hypercalcaemic type. *J Pathol* 238:389–400.
30. Comet I, Riising EM, Leblanc B, Helin K (2016) Maintaining cell identity: PRC2-mediated regulation of transcription and cancer. *Nat Rev Cancer* 16:803–810.
31. Kahali B, et al. (2014) The silencing of the SWI/SNF subunit and anticancer gene BRM in rhabdoid tumors. *Oncotarget* 5:3316–3332.
32. Rao Q, et al. (2015) Frequent co-inactivation of the SWI/SNF subunits SMARCB1, SMARCA2, and PBRM1 in malignant rhabdoid tumours. *Histopathology* 67:121–129.
33. Foulkes WD, et al. (2014) No small surprise—small cell carcinoma of the ovary, hypercalcaemic type, is a malignant rhabdoid tumour. *J Pathol* 233:209–214.
34. Reisman DN, Sciarrotta J, Wang W, Funkhouser WK, Weissman BE (2003) Loss of BRG1/BRM in human lung cancer cell lines and primary lung cancers: Correlation with poor prognosis. *Cancer Res* 63:560–566.
35. Herpel E, et al. (2017) SMARCA4 and SMARCA2 deficiency in non-small cell lung cancer: Immunohistochemical survey of 316 consecutive specimens. *Ann Diagn Pathol* 26:47–51.
36. Wilson BG, et al. (2014) Residual complexes containing SMARCA2 (BRM) underlie the oncogenic drive of SMARCA4 (BRG1) mutation. *Mol Cell Biol* 34:1136–1144.
37. Le Loarer F, et al. (2015) SMARCA4 inactivation defines a group of undifferentiated thoracic malignancies transcriptionally related to BAF-deficient sarcomas. *Nat Genet* 47:1200–1205.